CD27 is required for protective lytic EBV antigen specific CD8$^+$ T cell expansion

Yun Deng, Bithi Chatterjee, Kyra Zens, Hana Zdimerova, Anne Müller, Patrick Schumachers, Laure-Anne Ligeon, Antonino Bongiovanni, Riccarda Capaul, Andrea Zbinden, Angelika Holler, Hans Stauss, Wolfgang Hammerschmidt and Christian Münz

Supplementary Figure Legends

Figure S1. Related to Figure 1. Gating strategy of CD27$^+$ cells in huMice

(A) Representative flow cytometry gating strategy of CD27$^+$ cells in different immune cell populations in huMice.

Figure S2. Related to Figure 2. CD27 depletion effect on T and B cells

(A) Flow cytometry analysis of CD3$^+$ T cells -1 (before), 1 and 6 days post injection of anti-CD27 depletion antibody.

(B) Total numbers of CD19$^+$ B cells at the end of experiment as compared between anti-CD27 depletion antibody-treated group (n= 9-13 per group) and isotype control antibody-treated group (n= 8-11 per group). Mann-Whitney test was used to analyze the p value; ns: not significant. Data are pooled from two independent experiments.

Figure S3. Related to Figure 3. CD27 blocking antibody does not deplete CD27$^+$ cells, and no significant difference in EBV viral loads between groups with transferred BMLF1 and LMP2 specific T cells could be observed.

(A-B) Frequency of CD3$^+$ T cells (A) and CD19$^+$ B cells (B) in the respective group (left) and total cell count (right) in peripheral blood and spleen at termination of experiment.

(C) Graphical illustration describing the working principle of using two fluorochrome-conjugated anti-CD27 antibodies to check the blocking effect of the blocking antibody.

(D) Frequency of CD27$^+$ CD8$^+$ T cells detected by anti-CD27 antibody derived from a different clone to the injected anti-CD27 blocking antibody.

(E) Frequency of CD27$^+$ CD8$^+$ T cells detected by anti-CD27 antibody derived from the same clone as the injected anti-CD27 blocking antibody.

(F) Longitudinal data of animal weight over time until termination in the respective groups.

(G) Animal survival over time until experiment termination in the respective groups.

(H) Comparison of EBV viral loads in different transfer conditions in blood (left), spleen (middle) and liver (right).

(I) Frequency of CD27 positive of EBNA2$^+$ B cells in blood (left) and spleen (right).

(J) qRT-PCR analysis shows relative gene expression of the representative five EBV latent genes and five lytic genes in the anti-CD27 blocking antibody-treated group versus isotype control antibody treated group. Data are normalized to housekeeping gene SDHA expression. n= 4 from one out of three independent experiments.

(K-L) Representative immunohistochemistry images of EBNA2 in the respective groups, original magnification 200x (K), and the quantification of EBNA2$^+$ cells/mm^2 in splenic sections (L).

Data (n= 14-16 per group) are pooled from two independent mouse experiments in graph (A) and (C-H) and displayed with median and interquartile range. Two-way ANOVA analysis and Sidak's multiple comparisons as a post hoc test was used for (C -F) and (I), Mann-Whitney test for (A), two-way ANOVA analysis and Tukey's multiple comparisons for (H) to assess p values. Log-rank (Mantel-Cox) test for (G) was used to compare the survival curves. One-way ANOVA analysis (Kruskal-Wallis test) followed by Tukey's post hoc test was used for (L). Graph I (n=4-6 per group) is from one experiment and Mann-Whitney test was used to assess the p values: *$p<0.05$, **$p<0.01$, ***$p<0.001$. ns: not significant.

Figure S4. Related to Figure 4. Individual expression and co-expression of CD39, CD70, Ki67 and EBNA2 in blood and spleen under CD27 blockade

(A-B) UMAP presentation overlaid expression of each individual marker in blood (A) and spleen (B).

(C) Representative UMAP analysis depicts clusters, showing the co-expression of CD39, CD70, Ki67 and EBNA2 on the CD19$^+$ B cells in spleen.

(D) Transformed data from (C) are shown in frequency of each population in different experimental groups.

(E) Representative heatmap analysis of co-expression of CD39, CD70, Ki67 and EBNA2 on CD19$^+$ B cells in spleen.

Graphs (A-E) (n= 7-8 per group) are representative from one out of two independent experiments.

Figure S5. Related to Figure 5. Treatment with anti-CD27 blocking antibody shows no effect on T cell memory subsets *in vivo* and LCL proliferation *ex vivo*

(A) Comparison of T cell memory subsets characterized by CD45RA and CD62L expression and depicted as naïve, Tcm, Tem and Temra cells in different transfer conditions (BMLF1 and LMP2) in blood (from one representative experiment).

(B) T cell memory subsets in groups treated with either anti-CD27 blocking antibody or isotype control antibody *in vivo*. Cells were harvested at termination of experiment from spleen, liver and bone marrow.

(C) Flow cytometry plots of LCL proliferation. Three LCLs generated from human cells and huNSG/huNSG-A2 mice, respectively, were labeled with Cell Trace Violet and incubated with either anti-CD27 blocking antibody (10µg/mL) or isotype control antibody (10µg/mL) for 3 and 10 days.

Data (n=3 per group) in graph A is from one representative experiment. Data (n= 5-6 per group) in graph B are pooled from two independent experiments and displayed with median and interquartile range. Mann-Whitney test was used to assess p values; *$p<0.05$, **$p<0.01$.

Figure S6. Related to Figure 6.

(A) Overview of the CD20, CD8 and EBNA2 stainings in whole spleen sections after anti-CD27 blocking or isotype control antibody treatment, acquired by ChipCytometry. Big bright red and green spots in the isotype treatment condition are artifacts during acquisition.

(B) Frequency of $CD8^+$ T cells and $EBNA2^+CD20^+$ B cells as quantified in 5 to 7 randomly chosen positions.

(C) Immunofluorescence images for human CD45, CD7, CD38, the linage markers CD3, CD4, CD8, CD21 and CD11c.

(D) Immunofluorescence images for CD45RA, CD45RO and CD62L used to define T cell subsets.

(E) Immunofluorescence images for co-stimulatory/inhibitory molecules CD27, CD28, CD30, TIM3, CD278, CD40, CD134 (OX40 receptor) and the transcription factor FoxP3.

93 (F) Immunofluorescence images for CD39, HLADR, and Ki67.

94 Scale bars for (A), (C)-(F) are 50μm.

A

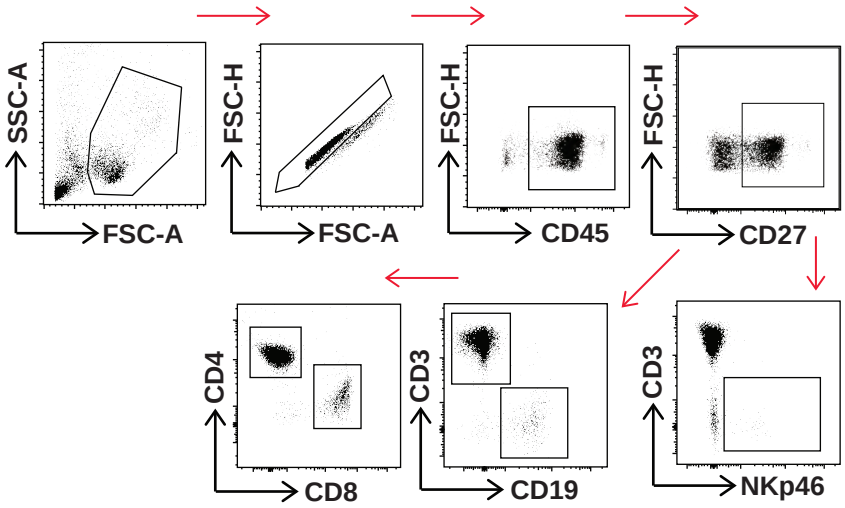
SSC-A
FSC-A
FSC-H
FSC-A
FSC-H
CD45
FSC-H
CD27
CD4
CD8
CD3
CD19
CD3
NKp46

Figure S1

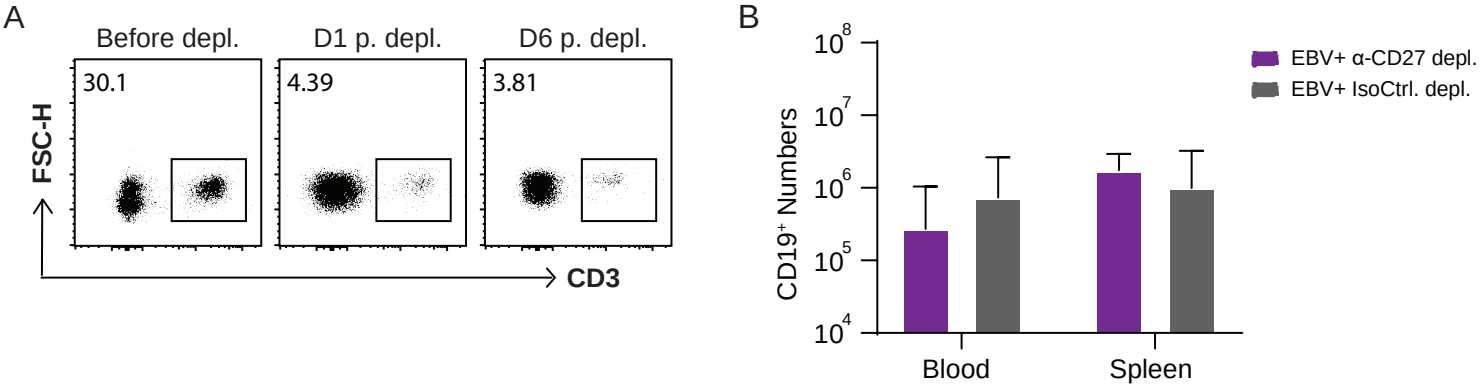
A
Before depl.
D1 p. depl.
D6 p. depl.
30.1
4.39
3.81
FSC-H
CD3
B
CD19+ Numbers
10^8
10^7
10^6
10^5
10^4
Blood
Spleen
EBV+ α-CD27 depl.
EBV+ IsoCtrl. depl.

Figure S2

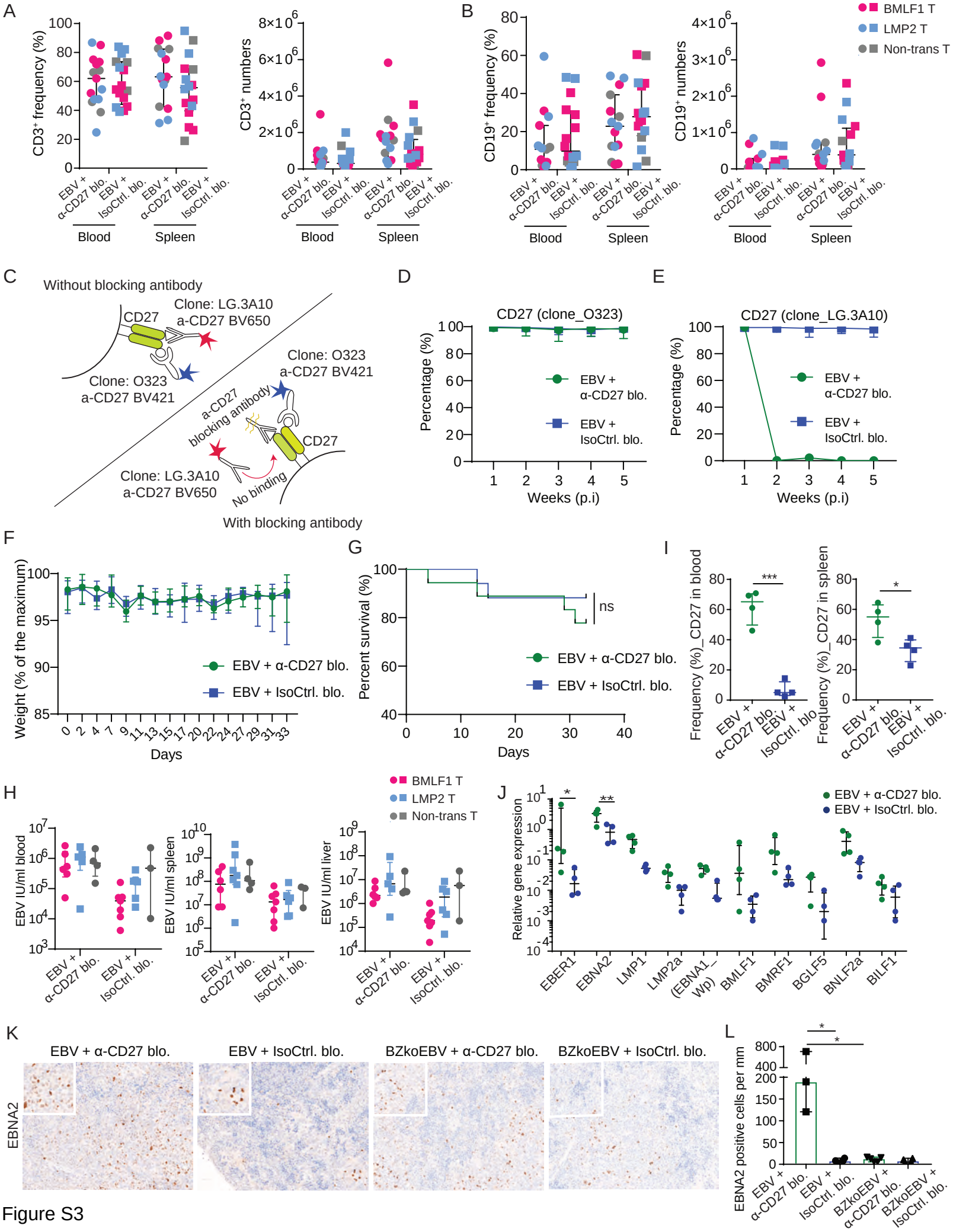
A
CD3+ frequency (%)
CD3+ numbers
B
CD19+ frequency (%)
CD19+ numbers
BMLF1 T
LMP2 T
Non-trans T
EBV + α-CD27 blo.
EBV + IsoCtrl. blo.
Blood
Spleen
C
Without blocking antibody
CD27
Clone: LG.3A10
a-CD27 BV650
Clone: O323
a-CD27 BV421
Clone: O323
a-CD27 BV421
a-CD27
blocking antibody
CD27
Clone: LG.3A10
a-CD27 BV650
No binding
With blocking antibody
D
CD27 (clone_O323)
Percentage (%)
Weeks (p.i)
E
CD27 (clone_LG.3A10)
F
Weight (% of the maximum)
Days
G
Percent survival (%)
ns
H
EBV IU/ml blood
EBV IU/ml spleen
EBV IU/ml liver
I
Frequency (%)_CD27 in blood
Frequency (%)_CD27 in spleen
J
Relative gene expression
EBER1
EBNA2
LMP1
LMP2a
(EBNA1_Wp)
BMLF1
BMRF1
BGLF5
BNLF2a
BILF1
K
EBV + α-CD27 blo.
EBV + IsoCtrl. blo.
BZkoEBV + α-CD27 blo.
BZkoEBV + IsoCtrl. blo.
EBNA2
L
EBNA2 positive cells per mm

Figure S3

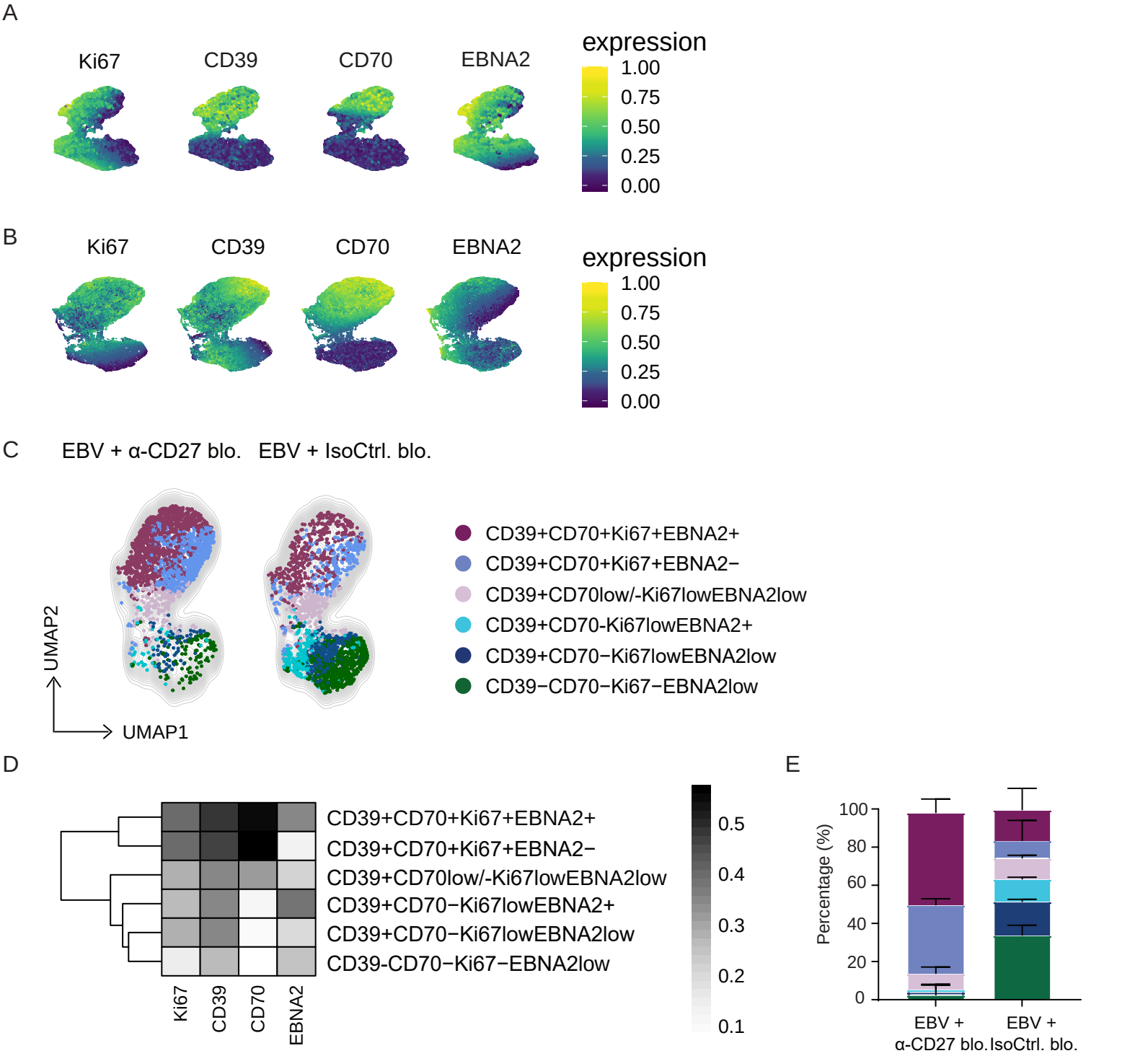
A
Ki67
CD39
CD70
EBNA2
expression
1.00
0.75
0.50
0.25
0.00
B
Ki67
CD39
CD70
EBNA2
expression
1.00
0.75
0.50
0.25
0.00
C
EBV + α-CD27 blo.
EBV + IsoCtrl. blo.
UMAP2
UMAP1
CD39+CD70+Ki67+EBNA2+
CD39+CD70+Ki67+EBNA2−
CD39+CD70low/-Ki67lowEBNA2low
CD39+CD70-Ki67lowEBNA2+
CD39+CD70−Ki67lowEBNA2low
CD39−CD70−Ki67−EBNA2low
D
CD39+CD70+Ki67+EBNA2+
CD39+CD70+Ki67+EBNA2−
CD39+CD70low/-Ki67lowEBNA2low
CD39+CD70−Ki67lowEBNA2+
CD39+CD70−Ki67lowEBNA2low
CD39-CD70−Ki67−EBNA2low
Ki67
CD39
CD70
EBNA2
0.5
0.4
0.3
0.2
0.1
E
Percentage (%)
100
80
60
40
20
0
EBV + α-CD27 blo.
EBV + IsoCtrl. blo.

Figure S4

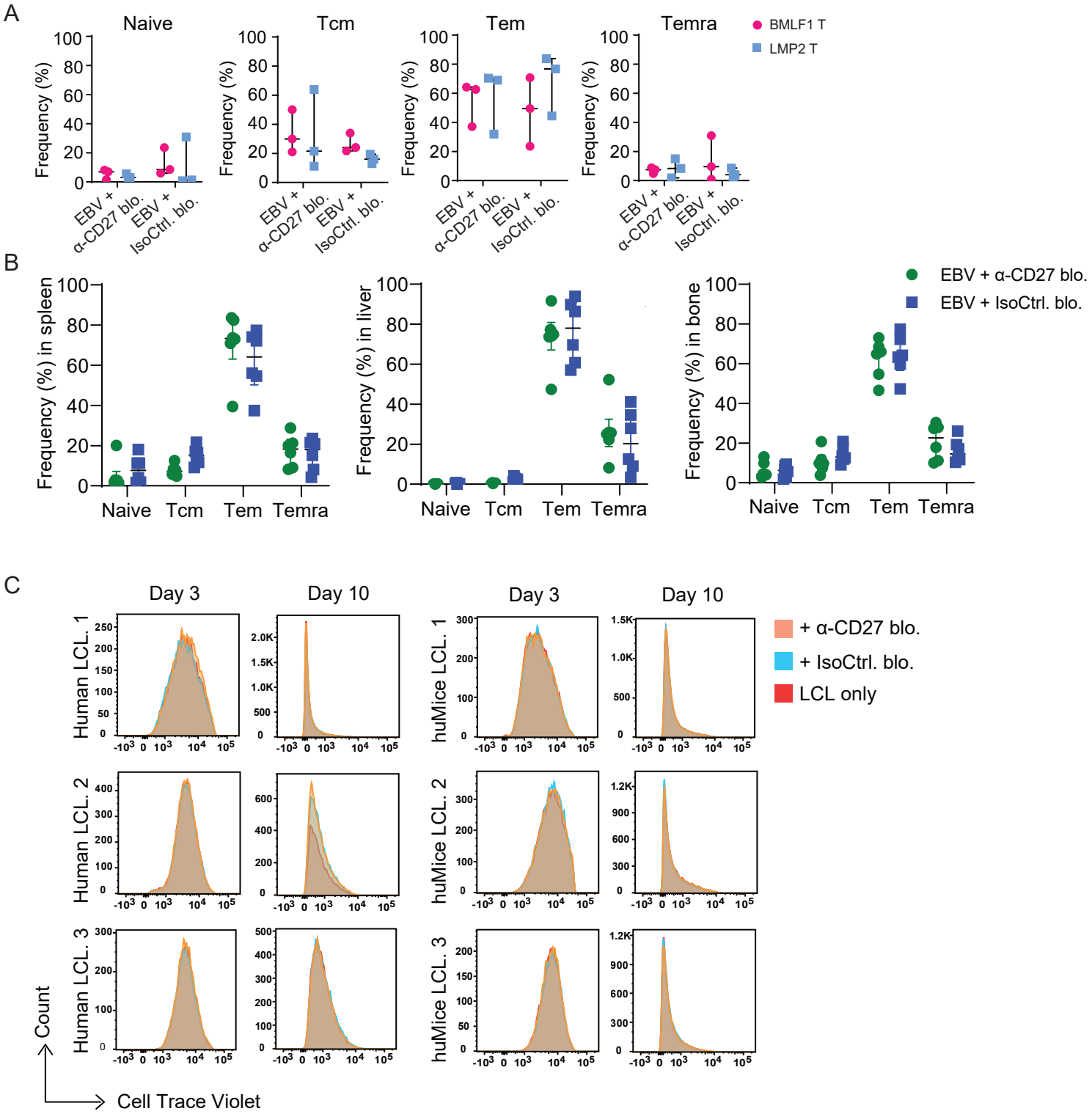
A
Naive
Tcm
Tem
Temra
BMLF1 T
LMP2 T
Frequency (%)
EBV + α-CD27 blo.
EBV + IsoCtrl. blo.
B
Frequency (%) in spleen
Frequency (%) in liver
Frequency (%) in bone
EBV + α-CD27 blo.
EBV + IsoCtrl. blo.
Naive
Tcm
Tem
Temra
C
Day 3
Day 10
Human LCL. 1
Human LCL. 2
Human LCL. 3
huMice LCL. 1
huMice LCL. 2
huMice LCL. 3
+ α-CD27 blo.
+ IsoCtrl. blo.
LCL only
Count
Cell Trace Violet

Figure S5

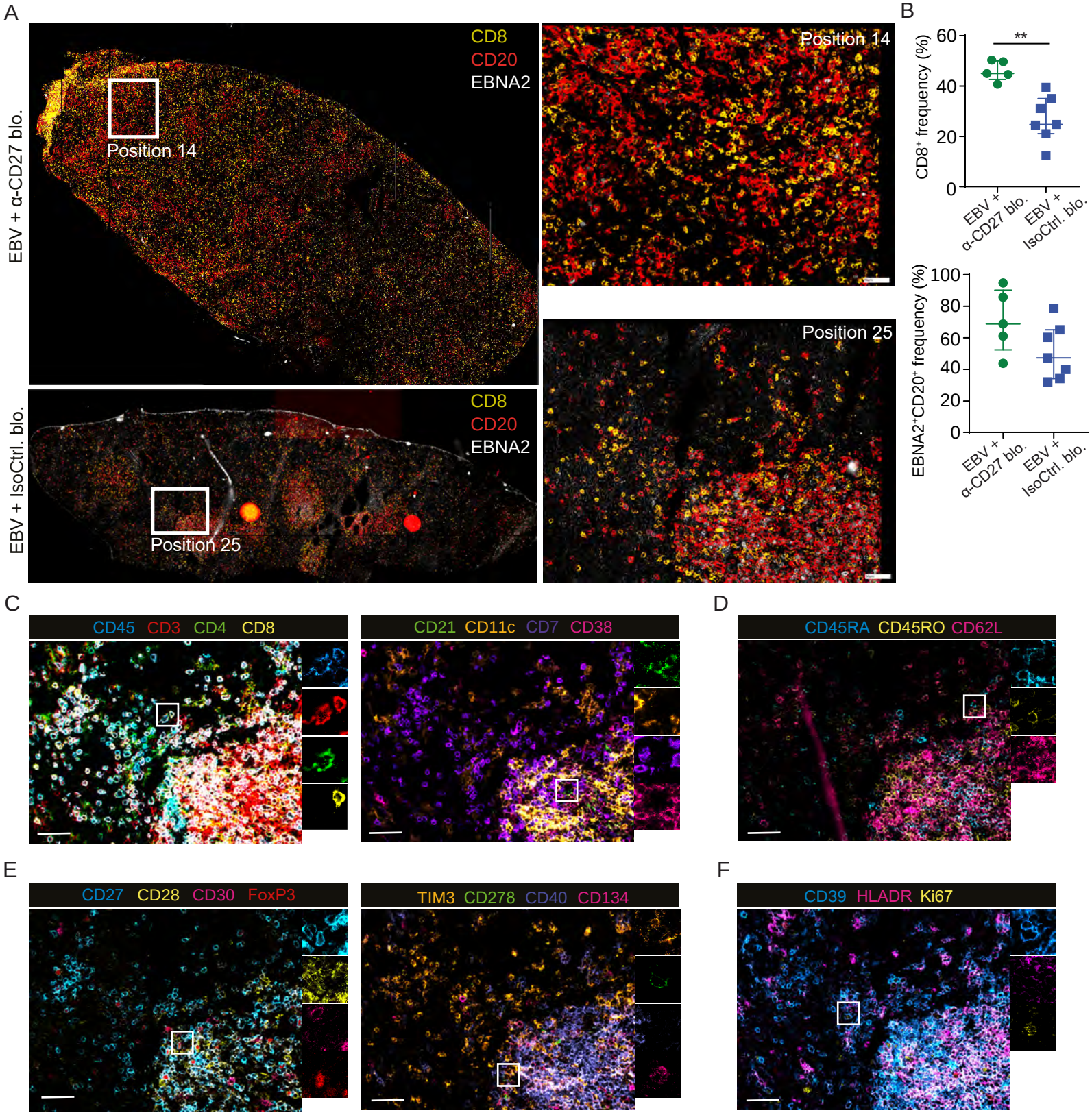
A
EBV + α-CD27 blo.
CD8
CD20
EBNA2
Position 14
Position 14
EBV + IsoCtrl. blo.
CD8
CD20
EBNA2
Position 25
Position 25
B
CD8+ frequency (%)
60
40
20
0
**
EBV + α-CD27 blo.
EBV + IsoCtrl. blo.
EBNA2+CD20+ frequency (%)
100
80
60
40
20
0
EBV + α-CD27 blo.
EBV + IsoCtrl. blo.
C
CD45 CD3 CD4 CD8
CD21 CD11c CD7 CD38
D
CD45RA CD45RO CD62L
E
CD27 CD28 CD30 FoxP3
TIM3 CD278 CD40 CD134
F
CD39 HLADR Ki67

Figure S6

Table S1: Antibodies and dyes for ChipCytometry

	Markers	Color	Clone	Company	Cat#
1	CD8	PerCP	SK1	Biolegend	344708
2	CD4	PE	RPA-T4	Biolegend	300508
3	CD45	BUV395	HI30	BD	563792
4	CD45RA	FITC	HI100	BD	555488
5	CD11c	PE	S-HCl-3	Biolegend	371504
6	CD27	PerCP	LG.3A10	Biolegend	124213
7	CD134 (OX40)	PE	Ber-Act35	Biolegend	350003
8	CD278 (ICOS)	PerCP	C398.4A	Biolegend	313517
9	CD45RO	FITC	UCHL1	BD	555492
10	CD3	PE	SK7	Biolegend	344805
11	CD56	PE	MEM-188	BL	304605
12	CD69	PE	FN50	Biolegend	310905
13	CD38	PE	HIT2	Biolegend	303506
14	CD30	PE	Ber-H8	BD	550041
15	CD20	PE	1412	Biolegend	340510
16	CD40	FITC	HB14	Biolegend	313004
17	CD7	FITC	CD7-6B7	Biolegend	343104
18	CD62L	PE	FMC46	BioRad	MCA1076PET
19	CD279 (PD1)	PE	EH12.1	BD	560795
20	HLA-DR	FITC	G46.6	BD	555811
21	CD28	PE	CD28.2	BD	5585729
22	CD21	PE	Bu32	Biolegend	354921
23	CD366 (TIM3)	PE	D5D5R	RD	FAB2365P
24	Ki67	PE	B56	BD	BD 556027
25	FOXP3	PE	236A/E7	BD	560852
26	CD39	FITC	A1	Biolegend	328207
27	EBNA2	PE	R3	Sigma	MABE8
28	Helix NP Green	FITC		Biolegend	425303

Table S2. Quantitative RT-PCR primer list in the paper.

Name	Primer/Probe	Source	Sequence
EBER1	F	Tierney et al., 2015	TGCTAGGGAGGAGACGTGTGT
	R		TGACCGAAGACGGCAGAAAG
	probe		AGACAACCACAGACACCGTCCTCACCA
EBNA2	F	Bell et al., 2006	GCTTAGCCAGTAACCCAGCACT
	R		TGCTTAGAAGGTTGTTGGCATG
	probe		CCCAACCACAGGTTCAGGCAAAACTTT
LMP1	F	Bell et al., 2006	AATTTGCACGGACAGGCATT
	R		AAGGCCAAAAGCTGCCAGAT
	pobe		TCCAGATACCTAAGACAAGTAAGCACCCGAAGAT
LMP2a	F	Bell et al., 2006	CGGGATGACTCATCTCAACACATA
	R		GGCGGTCACAACGGTACTAACT
	probe		CAGTATGCCTGCCTGTAATTGTTGCGC
EBNA1 (Wp)	F	Bell et al., 2006	TGCCTGAACCTGTGGTTGG
	R		CATGATTCACACTTAAAGGAGACGG
	probe		TCCTCTGGAGCCTGACCTGTGATCG
BMLF1	F	Tierney et al., 2015	CCCGAACTAGCAGCATTTCCT
	R		GACCGCTTCGAGTTCCAGAA
	probe		AACGAGGATCCCGCAGAGAGCCA
BMRF1	F	Tierney et al., 2015	GAGGAACGAGCAGATGATTGG
	R		TGCCCACTTCTGCAACGA
	probe		TGCTGTTGATGCCCAAGACGGCTT
BGLF5	F	Tierney et al., 2015	GCAAGCCCGGGAGAGACT
	R		GAGGCGACCGTTTTCGAA
	probe		CGGGTGAACATTGTGACGGCCTTC
BNLF2a	F	Tierney et al., 2015	TGGAGCGTGCTTTGCTAGAG
	R		GGCCTGGTCTCCGTAGAAGAG
	probe		CCTCTGCCTGCGGCCTGCC
BILF1	F	Tierney et al., 2015	TGCCTTTTGACCCAGAACATG
	R		CAACGCCATACCCAAGTGAGT
	probe		TACGGAGCACATCAGGCCCAAGAACA

Supplementary Methods

Humanized mouse generation and infection

NOD-scid γ_c^{null} (NSG) mice and HLA-A2 transgenic NSG mice were originally purchased from Jackson Laboratories (Bar Harbor, Maine, USA) and maintained in ventilated, specific pathogen-free cages at the Institute of Experimental Immunology, University of Zurich. To assist with the engraftment of human $CD34^+$ hematopoietic progenitor cells (HPCs), newborn pups (1-5 days) were irradiated with 1Gy prior to reconstitution [1,2]. Five to seven hours later, irradiated pups were intrahepatically injected with $2x10^5$ $CD34^+$ human hematopoietic progenitor cells (HPCs) isolated from human fetal livers (HFL) (Advanced Bioscience Resources, USA). The HFL samples were procured during termination between gestational weeks 14 and 22. Use of human tissue was approved by the cantonal ethics committee of Zurich (KEK-ZH-Nr. 2010-0057 and 2019-00837). After 12 weeks of reconstitution, peripheral blood was collected via tail vein bleeding and cells were checked for immune cell populations through expression of human CD45, CD3, CD4, CD8, CD19, NKp46 and HLA-DR, as previously described [3]. All procedures were strictly followed in accordance with the animal protocols ZH209/2014 & ZH159/17, licensed by the veterinary office of the canton of Zurich, Switzerland. Mice were immune phenotyped again prior to the start of the experiments and showed the following mean frequencies of different cell populations; $huCD45^+$ 81.5% ± 8.5%, $huCD3^+$ T cells of $huCD45^+$ 33.6% ± 10.9%, $huCD19^+$ B cells of $huCD45^+$ 53.9% ± 12.1%, $huCD4^+$ T cells of human T cells 74.5% ± 8.6%, $huCD8^+$ T cells of human T cells 22.4% ± 8.2% and $NKp46^+$ NK cells of $huCD45^+$ 3.2% ± 1.9%. Animals were used between 12 and 28 weeks old (Mean ± SD, n = 80; female 43 and male 37). Mice were then injected with 10^5 Raji Green units (RGU) of wild type Epstein Barr virus (EBV) or Luciferase-expressing EBV (Luc-EBV) intraperitoneally (i.p.) and monitored for 4 to 6 weeks. In each experimental group, 3 to 6 biological replicates were tested. For each individual experiment, animals were reconstituted from a single HFL donor and distributed into different experimental groups with a similar ratio of males and females, as well as similar reconstitution levels of human immune cell populations.

Wild type EBV, BZLF1 knock-out EBV and Luciferase-expressing EBV production

Wild type EBV B95-8 strain-producing cells were a generous gift of Prof. Dr. Henri-

Jacques Delecluse (DKFZ, Heidelberg, Germany). The recombinant EBV B95-8 DNA was stored as a bacmid and encompassed the gene for hygromycin resistance and green fluorescent protein (GFP) in HEK293 cells. Similarly, EBV B95-8-delta BZLF1 knock-out EBV (BZkoEBV) was produced in HEK293 cells. Those cells were cultured in DMEM (1X) medium supplemented with 10% heat inactivated FBS, 20µg/ml gentamycin and 20µg/ml hygromycin. Cell transfection was performed using 3 µg of BZLF1 (p509) and BALF4 (p2670) plasmids each, together with 32 µl of METAFECTENE® PRO (Biontex) in 10 cm petri dishes [3-5]. The virus supernatant was harvested 3 days after transfection and concentrated through centrifugation at 30,000g for 2 hours at 4 °C. Prior to animal infection, the GFP expressing virus was titrated on Raji cells *in vitro* by analyzing the GFP positive cells 48h after infection with flow cytometry. Based on the serial dilution of the virus on Raji cells, Raji Green units (RGU) were calculated for each virus preparation. Luciferase-expressing EBV (Luc-EBV) producer cells were kindly provided by Prof. Dr. Wolfgang Hammerschmidt (HelmholtzZentrum, Munich, Germany). Luc-EBV genome was originally derived from the B95-8 EBV with bioluminescent firefly luciferase protein incorporated as an EBV EBNA2 fusion construct and produced in HEK293 cells. It was produced and titrated in the same way as described above for wild type and BZLF1 knock-out EBV, if not stated otherwise.

EBV-specific T cell receptor (TCR) generation and adoptive T cell transfer

Phoenix-AMPHO packaging cells were transfected with envelope vector pCl-Ampho construct and either LMP2-TCR or BMLF1-TCR to produce retrovirus supernatants encoding EBV-specific TCRs. Subsequently, CD3/CD28 Dynabeads (Thermofisher Scientific) activated splenocytes derived from donor-mate animals were transduced with either LMP2-TCR or BMLF1-TCR encoding retroviruses. Transduction efficiency was determined by flow cytometry 48 hours after the second transduction. A total of 200’000 $TCR^{+}CD3^{+}$ T cells were transferred intravenously into donor-matched recipient mice and monitored longitudinally during the course of EBV infection.

***In vivo* bioluminescence imaging**

The progression of EBV infection was monitored longitudinally every week and quantitatively measured by *in vivo* bioluminescence imaging with the IVIS Spectrum

Imaging System (PerkinElmer). Animals were anesthetized by isofluorane with the flow of 3 liters per minute and injected i.p. with 150mg/kg D-Luciferin (Promega) 10 minutes before imaging. Mice were placed inside the IVIS imaging box and imaged dorsally and ventrally. Representative images were acquired at 2 minutes for each mouse during the entire experiment to illustrate the virus progression within the host. Images for quantification were captured at various time points before the luminescent signal reached the saturation intensity and analyzed with Living image 4.3.1 software (PerkinElmer). Regions of interest (ROI) were set to include the regions with luminescent signal in mice and photon flux (p/s) of light emitted per second within the ROI was measured as the readout.

Preparation of tissue sections for ChipCytometry

Splenic tissues from EBV infected mice treated with either anti-CD27 blocking antibody or the corresponding isotype control antibody were collected at the termination of experiment. Vertically dissected fresh tissues, up to 0.5cm in thickness were embedded in OCT (Tissue-Tek) and preserved at -80°C. Tissue sectioning was prepared on a cryostat (Leica) instrument by placing the frozen tissue block facing up on a freezing-temperature steel well and adjusting the temperature of the chamber and cutting knife to -16°C and -17°C, respectively. The section thickness was set to 5-6μm. Each individual section was collected on a room temperature microscope cover slide and assembled into a ZellSafe_T chip (Canopy Biosciences). Tissue on the cover slide was fixed using 100% acetone for 5 minutes, 90% ethanol for 3 minutes, 70% ethanol for 3 minutes on ice and washed twice with PBS.

Antibody staining and tissue immunofluorescence imaging in ChipCytometry

Prior to staining of the samples, individual antibodies were filtered and titrated to their optimal dilution to achieve a good signal-to-background staining, known as the optimal Fisher's discrimination ratio (FDR). Tissues on the chips were blocked using blocking buffer (1% fetal bovine serum, 10% normal mouse serum and 0.1% Tween-20 in PBS) for one hour at room temperature. For surface staining, the relevant monoclonal antibodies were prepared in 400μl of blocking buffer and incubated with the sample for 15 minutes at either four degrees or at room temperature, depending on the optimized staining condition per antibody. Followed by a continuous wash step with PBS containing 0.1% Tween-20 controlled by an automated Ismatec pump

system for 5 minutes and washing the chip twice with PBS, the chip was ready to be acquired. For the intranuclear staining, tissue was permeabilized using 1X perm buffer from the FoxP3 Transcription factor staining buffer set (Invitrogen), washed with PBS and incubated with antibodies for intranuclear markers for 15 minutes before washing. For the EBNA2 staining, tissue was blocked with blocking buffer containing 10% normal mouse serum, 1% FCS, 0.1% Tween 20 in 1X perm buffer for 1 hour. Purified primary EBNA2 rat anti-human antibody was applied in blocking buffer for 1 hour at 4°C. Followed by washing with 0.1% Tween 20, tissue was incubated with secondary mouse anti-rat IgG2a PE antibody (Biolegend) in blocking buffer for 15 minutes at room temperature, and then washed with PBS-0.1% Tween 20 before acquisition.

Combining Zellkraftwerk ZellScanner One and ZellExplorer software, fluorescent antibody-labeled tissue samples were acquired. Briefly, each chip was photobleached in all channels and scanned for background fluorescence. A whole slide scan was ordered in the beginning in order to have full spatial information about the tissue. After staining with the corresponding antibodies, the fluorescent signals were acquired and then photobleached preparing for the next round of acquisition of background fluorescence and fluorescent signals of antigens of interest. In the end, the net fluorescent signal was achieved and calculated by deducting the background fluorescence in each staining round. 28 parameters were assessed in the splenic tissue sections (Table S1).

Quantification of EBV DNA genome in blood and tissue

Total DNA from whole blood and small pieces of spleen and liver was extracted using NucliSENS easyMag (Biomerieux) and DNeasy Blood & Tissue Kit (QIAGEN) respectively, according to manufacturer's instructions. TaqMan (Applied Biosystems) real-time PCR was used to quantify EBV DNA as previously described [6], with modified primers for the BamH1 W fragment (50-CTTCTCAGTCCAGCGCGTTT-30 and 50-CAGTGGTCCCCCTCCCTAGA-30) and a fluorogenic probe (50-FAM CGTAAGCCAGACAGCAGCCAATTGTCAG-TAMRA-30). All samples were performed in duplicates and measured on either ViiA™ 7 Real-Time PCR System (ThermoFisher Scientific) or ABI Prism 7300 Sequence Detector (Applied Biosystems) at the Institute of Medical Virology, University of Zurich. Samples below the lower limit of quantification (LLOQ) of 122

International Units (IU)/ml were defined as negative for EBV DNA. EBV-inoculated animals with blood and splenic EBV DNA genome below the LLOQ were considered non-infected and excluded from further analysis.

Cell isolation and tissue preparation

Peripheral blood cells were obtained from the animals by tail vein bleeding and lysed with 1xACK lysis buffer for 5 minutes, followed by washing with PBS. Splenocytes were prepared as described above. Liver tissues were mechanically chopped into small pieces and enzymatically digested in 2ml of digestion buffer (1mg Collagenase D (Roche) and 0.2mg DNase I (Roche) in 2ml DMEM) at 37°C for 30 minutes with agitation. Dissociated livers were then passed through a 70μm cell strainer and subjected to centrifugation in a discontinuous Percoll gradient (40% and 70%, Sigma-Aldrich) for 20 minutes at 1000rpm. Cells aggregated at the interface between 40% and 70% Percoll gradient were harvested and washed twice with PBS. Bone marrow cells were flushed out of the femur by short centrifugation. Cells were washed with PBS and passed through a 70μm cell strainer if necessary. Cells from different organs were counted using the Beckman Coulter AcT diff Analyzer to aliquot the optimal number of cells for staining and calculation of the total cell numbers for different experimental purposes.

Antibody, pentamer labeling and flow cytometry

Surface staining was performed by incubating cells with the relevant mAbs for 20 minutes at 4°C, followed by washing with PBS twice and resuspending in fixation buffer (1% paraformaldehyde) before acquisition. For intracellular staining, cells were labeled with mAbs against surface markers and fixed in fixation buffer as stated above. Then, cells were permeabilized by two washes with PBS+0.05% saponin (PS), resuspended with mAbs against intracellular markers diluted in PS and incubated for 20 minutes at 4°C. For intranuclear staining, cells labeled with mAbs against surface markers were fixed and permeabilized with Foxp3/Transcription Factor Staining Buffer Set (eBioscience) and stained with mAbs against intranuclear markers for 1 hour at 4°C. To detect EBV specific $CD8^+$ T cells, PE-conjugated pentamers specific for BMLF1 and LMP2 antigens, restricted by HLA-A*0201 (Proimmune), were incubated with the cells prior to surface staining for 10 minutes at room temperature [2]. Labeled cells were acquired on either the BD FACSCantoII, BD LSRFortessa or BD

FACSymphony. The data analysis was performed using FlowJo software (FlowJo LLC).

In vitro-transformed LCL generation

To generate NSG LCLs *ex vivo*, $CD19^+$ B cells were isolated from the spleen using positive selection with CD19 microbeads according to the manufacturer's recommendations (Miltenyi Biotec). A total of $5x10^5$ cells/well were plated in a 96-well U-bottom plate and cultured with EBV supernatants with a MOI of 0.5. Cells were cultured in RPMI 1640 medium supplemented with 10% heat inactivated FBS, 50U/ml penicillin-streptomycin and 1% L-glutamine. Cell growth was monitored by light microscopy and clusters of cells were normally visible 2 weeks post EBV infection. Outgrowing cells were further expanded by seeding at $3\text{-}5x10^5$ cells/ml and splitting at a concentration of 10^6 cells/ml.

Generation of EBV specific $CD8^+$ T cell clones and T cell re-stimulation

EBV specific T cell clones for BMLF1 and LMP2 were generated from a healthy HLA-A*0201 positive EBV carrier using BMLF1 and LMP2-specific dextramers, as described previously [3]. Briefly, dextramer positive $CD8^+$ T cells were single-cell sorted and co-cultured with irradiated autologous LCLs and PBMC feeder cells in complete T cell medium supplemented with 1µg/ml PHA and 150U/ml IL-2 [7]. IFNγ secretion was analyzed upon re-stimulation with 1µM of the relevant peptides using enzyme-linked immunosorbent assays (ELISA; MABTECH). Only the T cells, which showed specific responses to the relevant peptide were used for further phenotypic characterization and functional T cell avidity tests in peptide titration assays to confirm the specificity of the respective clones.

For re-stimulation, autologous LCLs were pulsed with either BMLF1 or LMP2 specific peptide (1µM), PBMC feeder cells were stimulated with PHA (5µg/ml) overnight and they were irradiated at 20Gy and 60Gy, respectively. T cell clones specific for BMLF1 and LMP2 were co-cultured with irradiated LCLs and PBMC feeder cells at the ratio of 1:5:50 in complete T cell medium (as stated above) for stimulation and expansion for 1 to 2 weeks before conducting the described experiments.

In vitro cytotoxicity assay

Cytotoxic activity of BMLF1 and LMP2 specific T cell clones against autologous LCLs was evaluated as previously described [1]. In brief, target cells (LCLs) were labeled with PKH-26 (Sigma-Aldrich) for 5 minutes and washed with PBS according to the manufacturer's instructions. T cells, pretreated with either anti-CD27 blocking antibody or the corresponding isotype control antibody for a week at the concentration of 5μg/ml, were co-cultured with the labeled target cells at 10:1, 1:1 and 1:10 effector/target ratios. After 21 hours of incubation, TO-PRO-3-iodide (ThermoFisher Scientific), a membrane-impermeable nuclear counterstain for dead cells, was added to each culture (0.5μM final concentration) and cells were analyzed by flow cytometry. Background and maximum TO-PRO-3-iodide staining was obtained by incubation of target cells with medium and/or heating the cells at 90°C for 15 minutes, respectively. The percentage of specific lysis was calculated with the following formula: ((%TO-PRO-3-iodide$^+$PKH26$^+$ cells in co-culture - %TO-PRO-3-iodide$^+$PKH26$^+$ cells in medium) / (%TO-PRO-3-iodide$^+$PKH26$^+$ cells in max kill - %TO-PRO-3-iodide$^+$PKH26$^+$ cells in medium)) x 100%.

Histology, immunohistochemistry and immunofluorescence

Tissue sections were excised and fixed in 4% formalin overnight before paraffin embedding (SophistoLab). For immunohistochemistry and immunofluorescence, tissue was prepared in 3μm sections with Leica BOND-MAX or Bond-III automated immunohistochemistry system. Tissue sections were treated with BOND Epitope Retrieval Solution 2 (Leica Biosystem) for antigen retrieval at 100°C for 30 minutes. Stainings were performed with Leica HRP Refine Kit (Leica Biosystem). Briefly, samples were incubated with mAb mouse anti-EBNA2 (Abcam) for 30 minutes, followed by incubation with Post Primary Rabbit anti mouse IgG for 20 minutes and anti-rabbit Poly-HRP-IgG for 15 minutes. 3,3'-Diaminobenzidine tetrahydrochloride (DAB) was the substrate chromogen used to visualize the complex via brown precipitate and hematoxylin counterstaining was performed for the visualization of cell nuclei. All stainings were acquired with a Vectra3 automated quantitative pathology imaging system (PerkinElmer) and analyzed with InForm software to quantify positive staining [8].

Serum cytokine quantification

Serum samples harvested from cardiac puncture at the termination of experiments were preserved at -20°C until use. Concentration of each individual cytokine (prepared 1:2.5 with dilution buffer) were measured in duplicates using V-PLEX Proinflammatory Panel 1 kits (Mesoscale) following the manufacturer's instructions. Standard dilutions for the calibrator blend for standard curve generation were prepared in parallel in duplicates. Plates were read with a Meso Quickplex SQ120 and analyzed with Discovery Workbench 4.0.12 (Mesoscale) [2,9].

B cell isolation and quantitative RT-PCR (qRT-PCR)

Total RNA was isolated with MACS sorting for B cells using CD19 human MicroBeads (Miltenyi Biotec) and extracted using RNeasy Mini Kit (QIAGEN) according to the manufacturer's recommendations. To avoid genomic DNA contamination, the on-column DNase processing was included during the RNA isolation (RNase-Free DNase Set, QIAGEN). cDNA was synthesized in a 20µl volume mixed with reverse transcriptase (Promega) and primer mix at concentrations of 10µM each. qRT-PCR was performed with a CFX384 Touch Real-Time PCR Detection System (Bio-Rad) using a program of 2 minutes at 50°C and 10 minutes at 95°C, followed by 50 cycles of amplification (95°C for 15 seconds and 60°C for 1 minute) [9]. Primers used in this manuscript are listed in Table S2 [10,11]. Transcript level of each gene of interest was calculated relative to the geometric mean of the reference gene *SDHA* (TaqMan Applied Biosystems Gene Expression Assay (Hs00417200)) and presented as relative gene expression.

Fluorescence image segmentation and quantification

Quantification of cells positive for EBNA2, CD8, CD20, CD69 and PD1 (single and/or double-positive) was performed using a homemade semiautomatic plugin designed on ImageJ. For every image the channels were separated and cell segmentation were performed on the nuclei channels, then the average of fluorescence intensity for each single protein was measured (the threshold is selected manually for each channel), and followed by quantification. The lineage markers and markers that are expressed on many different types of immune cells are show in Figure S6C; the markers used to characterize the T cell subsets are shown in Figure S6D; the stainings for co-stimulatory molecules and their receptors, as well as FoxP3 that are all positive

for CD27 are shown in Figure S6D; the markers that have high expression on B cells are shown in Figure S6F.

High-dimensional analysis

Flow cytometry data was processed using FlowJo software and imported into Cytobank to generate cell density plots and histograms (Beckman Coulter). All the parameters were displayed with an arcsinh transformation with an argument ranging from 50 to 500 on different biomarkers. The exported FCS files, together with the argument information, were uploaded into Rstudio. The FlowSom algorithm was used for automated clustering of cell populations for UMAP and heatmap [12]. Individual cluster frequencies generated in the R environment were exported and used for further analysis.

References

1. Strowig T, Gurer C, Ploss A, et al. Priming of protective T cell responses against virus-induced tumors in mice with human immune system components. *J Exp Med*. 2009;206(6):1423-1434.

2. Chatterjee B, Deng Y, Holler A, et al. $CD8^+$ T cells retain protective functions despite sustained inhibitory receptor expression during Epstein-Barr virus infection in vivo. *PLoS Pathog*. 2019;15:e1007748.

3. Antsiferova O, Müller A, Rämer P, et al. Adoptive transfer of EBV specific $CD8^+$ T cell clones can transiently control EBV infection in humanized mice. *PLoS Pathog*. 2014;10(8):e1004333.

4. Chijioke O, Muller A, Feederle R, et al. Human natural killer cells prevent infectious mononucleosis features by targeting lytic Epstein-Barr virus infection. *Cell Rep*. 2013;5(6):1489-1498.

5. Nowag H, Guhl B, Thriene K, et al. Macroautopphagy proteins assist Epstein Barr virus production and get incorporated into the virus particles. *EBioMedicine*. 2014;1(2-3):116-125.

6. Berger C, Day P, Meier G, Zingg W, Bossart W, Nadal D. Dynamics of Epstein-Barr virus DNA levels in serum during EBV-associated disease. *J Med Virol*. 2001;64(4):505-512.

7. Fonteneau JF, Larsson M, Somersan S, et al. Generation of high quantities of viral and tumor-specific human $CD4^+$ and $CD8^+$ T-cell clones using peptide pulsed mature dendritic cells. *J Immunol Methods*. 2001;258(1-2):111-126.

8. Murer A, McHugh D, Caduff N, et al. EBV persistence without its EBNA3A and 3C oncogenes in vivo. *PLoS Pathog*. 2018;14(4):e1007039.

9. McHugh D, Caduff N, Barros MHM, et al. Persistent KSHV infection increases EBV-associated tumor formation in vivo via enhanced EBV lytic gene expression. *Cell Host & Microbe*. 2017;22(1):61-73.

10. Tierney RJ, Shannon-Lowe CD, Fitzsimmons L, Bell AI, Rowe M. Unexpected patterns of Epstein-Barr virus transcription revealed by a high throughput PCR array for absolute quantification of viral mRNA. *Virology*. 2015;474:117-130.

11. Bell AI, Groves K, Kelly GL, et al. Analysis of Epstein-Barr virus latent gene expression in endemic Burkitt's lymphoma and nasopharyngeal carcinoma tumour cells by using quantitative real-time PCR assays. *J Gen Virol*. 2006;87(Pt 10):2885-2890.

12. Nowicka M, Krieg C, Crowell HL, et al. CyTOF workflow: differential discovery in high-throughput high-dimensional cytometry datasets. *F1000Res*. 2017;6:748.